0026-895X/09/7601-125–133$20.00
MOLECULAR PHARMACOLOGY
Copyright © 2009 The American Society for Pharmacology and Experimental Therapeutics
Mol Pharmacol 76:125–133, 2009

Vol. 76, No. 1
55657/3482855
Printed in U.S.A.

S3b Amino Acid Substitutions and Ancillary Subunits Alter the Affinity of *Heteropoda venatoria* Toxin 2 for Kv4.3

Christopher V. DeSimone, YiChun Lu, Vladimir E. Bondarenko, and Michael J. Morales

Department of Physiology & Biophysics, University at Buffalo, the State University of New York, Buffalo, New York (C.V.D., Y.C.L., M.J.M.); and Department of Mathematics and Statistics, Georgia State University, Atlanta, Georgia (V.E.B.)

Received February 16, 2009; accepted April 8, 2009

ABSTRACT

Heteropoda venatoria toxin 2 (HpTx2) is an inhibitor cystine knot (ICK)-gating modifier toxin that selectively inhibits Kv4 channels. To characterize the molecular determinants of interaction, we performed alanine scanning of the Kv4.3 S3b region. HpTx2-Kv4.3 interaction had an apparent K_d value of 2.3 μM. Two alanine mutants in Kv4.3 increased K_d values to 6.4 μM for V276A and 25 μM for L275A. Simultaneous mutation of both amino acids to alanine nearly eliminated toxin interaction. Unlike Hanatoxin and other well characterized ICK toxins, HpTx2 binding does not require a charged amino acid for interaction. To determine whether the identity of the S3b binding site amino acids altered HpTx2 specificity, we constructed Kv4.3 [LV275IF]. This mutation decreased the K_d value to 0.54 μM, suggesting that the hydrophobic character of the putative binding site is the most important property for interaction with HpTx2. One mutant, N280A, caused stronger interaction of HpTx2 with Kv4.3; the K_d value for Kv4.3 [N280A] was 0.26 μM. To understand Kv4.3-based transient outward currents in native tissues, we tested the affinity of HpTx2 for Kv4.3 coexpressed with KChIP2b. The toxin's K_d value for Kv4.3 + KChIP2b was 0.95 μM. KChIP2b stabilizes the closed state of Kv4.3, suggesting that the increased toxin affinity is due to increased stabilization of the closed state. These data show that HpTx2 binding to Kv4.3 has aspects in common with other ICK gating modifier toxins but that the interventions that increase toxin affinity suggest flexibility toward channel binding that belies its unusual specificity for Kv4 channels.

Voltage-gated K^+ channels of the Kv4 (*Shal*) family are present in many mammalian tissues, most prominently in the heart and central nervous system. Like several voltage-gated K^+ channels, their currents are transient and are characterized by rapid activation and inactivation. However, among channels that show similar kinetics, Kv4 channels are characterized by their unusually fast kinetics of recovery from inactivation (Birnbaum et al., 2004). In the hearts of most mammals, these channels are responsible for the fast-recovering transient outward K^+ current (I_{to}) (Birnbaum et al., 2004; Patel and Campbell, 2005). In the central nervous system, Kv4 channels are responsible for the I_A current in the somatodendritic region of neurons (Jerng et al., 2004). Currents generated by Kv4 channels are also found in the smooth muscle of the lower gastrointestinal tract, uterine wall, and vasculature (Birnbaum et al., 2004). Because of their central role in many important physiological processes, Kv4 channels are promising targets for drug development (Wickenden, 2002; Nattel and Carlsson, 2006).

Kv4 channel activity is modulated by several types of ancillary subunits (Birnbaum et al., 2004), the most prominent of which are the Kv4 channel-interacting proteins (KChIPs), a family of cytoplasmic calcium binding proteins ranging from 184 to 285 amino acids in humans. The products of three KChIP genes are predominant in the central nervous system (KChIPs 1, 3, and 4), whereas KChIP2 is more abundant in the heart, in where it contributes to the cardiac I_{to} (Patel and Campbell, 2005). KChIPs interact with the N terminus and T1 domains of Kv4 channels, in which they serve as chaperones to increase the expression of α subunits, modulate channel-gating kinetics, and alter the pharmacological properties of Kv4 channels (Birnbaum et al., 2004; Bett et al., 2006; Covarrubias et al., 2008; Maffie and Rudy, 2008).

One pharmacological modulator of Kv4 channels is HpTx2, a 33-amino acid peptide toxin originally purified from the venom of the spider *Heteropoda venatoria* (Sanguinetti et al.,

This work was supported by a Scientist Development Grant and Predoctoral Fellowship from the Founders Affiliate of the American Heart Association [Grants 0235500T, 0615662T]; the John R. Oishei Foundation; and the National Institutes of Health National Heart, Lung, and Blood Institute [Grant HL52874].

Parts of this work were presented at the Joint Meeting of the Biophysical Society 52nd Annual Meeting and 16th International Biophysics Congress, 2–6 Feb 2008, Long Beach, CA; and in thesis form at the University at Buffalo, the State University of New York.

Article, publication date, and citation information can be found at http://molpharm.aspetjournals.org.

doi:10.1124/mol.109.055657.

ABBREVIATIONS: KChIP, Kv4 channel-interacting protein; HpTx2, *Heteropoda venatoria* toxin 2; HaTx, hanatoxin; WT, wild type; ICK, inhibitor cystine knot; BSA, bovine serum albumin; SGTx, *Scodra griseipes* toxin.

1997). It is one of a diverse group of peptide toxins that form an "inhibitor cystine knot" (ICK) motif (Norton and Pallaghy, 1998). HpTx2 and the nearly identical HpTx3 have been shown to inhibit Kv4-based transient outward currents in the hearts and brains of several mammalian species but to have no apparent effect on other currents, including non-Kv4-based transient K^+ currents, demonstrating the toxin's utility in understanding native transient outward potassium currents (Sanguinetti et al., 1997; Brahmajothi et al., 1999; Guo et al., 1999, 2005; Himmel et al., 1999; Kassiri et al., 2002; Ramakers and Storm, 2002; Sanchez et al., 2002; Varga et al., 2004; Aimond et al., 2005; Tang et al., 2005; Lauver et al., 2006; Wang and Schreurs, 2006; Wang et al., 2006; Colinas et al., 2008; Nerbonne et al., 2008).

We have shown previously that recombinant HpTx2 is specific for Kv4 channels over Kv1.4, Kv2.1, and Kv3.4. Recombinant HpTx2 inhibits Kv4.3 current in a voltage-dependent manner. It shifts the threshold for activation to more depolarized voltages, speeds deactivation, and slows inactivation. This gating modification occurs through binding externally exposed portions of the voltage-sensor domain (Zarayskiy et al., 2005). However, the precise positions of amino acids responsible for HpTx2–Kv4.3 interaction were not identified, and the mechanism of the interaction was not revealed. In this article, we analyzed a series of Kv4.3 S3b alanine mutants' response to HpTx2. These experiments showed that leucine 275 and valine 276 are critical for HpTx2 inhibition of Kv4.3. These amino acids are in a position identical with that of the isoleucine and phenylalanine shown to be required for hanatoxin (HaTx) binding to Kv2.1 (Swartz and MacKinnon, 1997b). However, unlike HaTx, HpTx2 does not require a charged amino acid for interaction with Kv4.3. We also identified an alanine substitution, N280A, that increased affinity of Kv4.3 for HpTx2 nearly 10-fold. Mutation of Leu275 and Val276 to isoleucine and phenylalanine, respectively, increased the degree of HpTx2-induced gating modification, suggesting that hydrophobic interactions are the key for HpTx2 interaction. To understand better the behavior of Kv4.3-based transient currents in native tissues, we tested the affinity of HpTx2 for Kv4.3 coexpressed with KChIP2b. The toxin had a 2-fold higher affinity for Kv4.3+KChIP2b than Kv4.3 alone, suggesting that stabilization of the closed state of Kv4.3 also increases toxin affinity. These data lead to a view that highly specific interaction of HpTx2 with a Kv4.3 requires a very simple binding site and that the degree of gating modification can be modulated by ancillary subunits that alter the gating properties of Kv4.3.

Materials and Methods

Preparation of RNA for Oocyte Injection. The short form of rat Kv4.3 (636 amino acids; National Center for Biotechnology Information accession NP_113927) and KChIP2b, the 270-amino acid form (isoform 2) of KChIP2 (AAL51037) were described previously (Patel et al., 2002; Li et al., 2006). Plasmids encoding cloned channels and a phage RNA polymerase promoter were linearized by restriction endonuclease digestion and transcribed using T7 RNA polymerase (mMESSAGE mMACHINE; Ambion, Austin, TX). The reaction was terminated by DNAase I treatment followed by precipitation of RNA with LiCl and suspended in RNAase-free water. The sample concentration was determined by absorbance at 260 nm, adjusted to 500 ng/ml, and stored at −80°C.

Site-Directed Mutagenesis. Polymerase chain reaction-based mutagenesis was performed as described previously (Zarayskiy et al., 2005). Each mutant required two oligonucleotides encoding the desired mutation that overlapped by 12 nucleotides and were at least 30 nucleotides in length. Separate 25-μl reactions each contained 1× *Pfu* buffer, 1 unit of *Pfu* DNA polymerase (Stratagene, La Jolla, CA), 0.2 μg of template plasmid, and 40 μM each of the 4 dNTPs. Each reaction had 0.1 μg of one mutagenic primer and was subjected to 4 cycles of 94°C for 30 s, 55°C for 60 s, and 68°C for 6 min. The reactions were mixed, and cycling was repeated with 12 additional cycles. The completed reaction was digested with DpnI and transformed into *Escherichia coli*. Mutants were confirmed by DNA sequencing.

HpTx2 Synthesis. Toxin was produced by heterologous expression in *E. coli* as described previously (Zarayskiy et al., 2005). Its amino acid sequence is identical with native HpTx2 purified from *H. venatoria* (Sanguinetti et al., 1997) except for two additional amino acids (glycine-serine) on its amino terminus; we previously referred to this recombinant toxin as $rHpTx2_{GS}$ (Zarayskiy et al., 2005).

***Xenopus laevis* Oocyte Preparation.** Use of *X. laevis* was considered and approved for the numbers of animals, humane treatment, and care by the University at Buffalo-SUNY Institutional Animal Care and Use Committee and was carried out in accordance with the Declaration of Helsinki and with the Guide for the Care and Use of Laboratory Animals (Institute of Laboratory Animal Resources, 1996). Oocytes were prepared as described previously (Li et al., 2006). Frogs obtained from Xenopus I (Dexter, MI) were anesthetized by immersion in 3-aminobenzoic acid ethyl ester for 10 to 60 min. The ovarian lobes were harvested and placed in Ca^{2+}-free ND96 (96 mM NaCl, 2 mM KCl, 1 mM $MgCl_2$, and 5 mM HEPES, pH 7.4) and treated with 1 to 2 mg/ml collagenase (Type II; Sigma-Aldrich, St. Louis, MO) to remove the follicular cell layer. Oocytes were injected with 10 to 50 nl of in vitro-transcribed mRNA; when necessary, KChIP2b mRNA was injected at a 1:1 ratio KChIP2b:Kv4.3 (w/w). Injected oocytes were incubated at 18°C in normal ND96 (including 1.8 mM $CaCl_2$) + antibiotic/antimycotic (Invitrogen, Carlsbad, CA) for 3 to 7 days.

Two-Electrode Voltage-Clamp Technique. Currents were measured in oocytes using a two-microelectrode Dagan CA-1B amplifier as described previously (Wang et al., 2004). Expression of KChIP2b was established by the faster recovery from inactivation than that shown by Kv4.3 alone (Wang et al., 2002; Li et al., 2006). Electrodes were filled with 3 M KCl. Experiments were performed at room temperature (20–24°C) in either ND96 + 0.1% BSA or 98K + 0.1% BSA (98 mM KCl, 1 mM $MgCl_2$, 1.8 mM $CaCl_2$, and 5 mM HEPES, pH 7.4). Data were digitized at either 50 or 5 kHz using pClampex 9.2 (Molecular Devices, Sunnyvale, CA) and analyzed with pClampfit 9.2 (Molecular Devices), Microsoft Excel 2007 (Microsoft, Redmond, WA), or SigmaPlot 9 (Systat Software, Inc., San Jose, CA). Raw traces shown were neither leakage- nor capacitance-subtracted.

After performing control pulse protocols, toxin was applied to the oocyte-containing flow cell as a 2× solution and mixed by gentle pipetting. Subsequent protocols were applied without perfusion, except for washouts. Lack of perfusion did not cause current inhibition due to external K^+ accumulation, because we identified mutants that did not interact with the toxin and were not inhibited during these protocols (Fig. 6).

A two-pulse protocol was used to measure the voltage-dependence of G/G_{max} and steady-state inactivation relationships. From a holding potential of −90 mV, 18 3-s voltage steps (P1) were applied from −120 to +50 mV in 10-mV increments followed by a 1-s pulse (P2) to +50 mV. Conductance $G(V)$ at each voltage was calculated from the equation $G(V) = I_{max1,Kv4.3}/(V - E_K)$, where V is the depolarization voltage during P1, $I_{max1,Kv4.3}$ is the maximum $I_{Kv4.3}$ current during P1, and $E_K = -100$ mV, the reversal potential in ND96 + 0.1% BSA. The voltage-dependence of G/G_{max} was obtained by normalization of $G(V)$ to the maximal conductance value G_{max}. Activation curves G/G_{max} were fitted by a Boltzmann function $f_a(V) = 1/(1 + \exp[(V_{1/2} - V)/k])$, where $V_{1/2}$ and k are the half-activation potential

and the slope, respectively. The G/G_{max} curves used to calculate the change in Gibbs free energy (ΔG) due to toxin application in Fig. 2G were calculated as $\Delta G_{0,+HpTx2} = RT[(V_{1/2}/k) - (V_{1/2,+HpTx2}/k_{+HpTx2})]$, where R is the gas constant and T is absolute temperature (RT = 0.582 kcal/mol) and $V_{1/2,+HpTx2}$ and k_{+HpTx2} are the half-activation potential and the slope after toxin application, respectively. The differences in $\Delta G_{0,+HpTx2}$ for WT and mutant channels were determined from the equation $\Delta\Delta G_0 = \Delta G_{0,WT+HpTx2} - \Delta G_{0,mutant+HpTx2}$. Positive $\Delta\Delta G_0$ values represent decreased gating modification induced by HpTx2, whereas negative values represent increased gating modification; these values are included in Table 1. Apparent K_d values were also used to calculate the ΔG_0 due to toxin binding from the equation $\Delta G_0 = RT(\ln(K_d))$. Steady-state inactivation relationships were determined as the ratio of the maximum of $I_{Kv4.3}$ during P2, $I_{max2,Kv4.3}$, for the depolarization voltage during P1 to the maximum value of $I_{max2,Kv4.3}$, $I_{max2,Kv4.3}$ ($V = -120$ mV). Steady-state inactivation relationships were fitted by the Boltzmann function $f_i(V) = 1/(1 + \exp[(V_{1/2,i} - V)/k_i])$, where $V_{1/2,i}$ and k_i are the half-inactivation potential and the slope, respectively.

Results

We have shown previously that recombinant HpTx2 is specific for Kv4 channels over Kv1.4, Kv2.1, and Kv3.4 (Zarayskiy et al., 2005). Recombinant HpTx2 inhibits Kv4.3 current in a voltage-dependent manner. It shifts the threshold for activation to more depolarized voltages, speeds deactivation, and slows inactivation. HpTx2 failed to inhibit the gating of a Kv4.3 mutant in which the S3b-S4 linker region of Kv4.3 was replaced with that of Kv1.4, a K^+ channel whose gating is unaffected by HpTx2 (Zarayskiy et al., 2005). This externally exposed region is near the gating modifier "hot spot" for interaction of ICK toxins with the voltage sensor domain of voltage-gated ion channels (Swartz, 2007).

The Putative Binding Site of HpTx2 Is in S3b. To determine which amino acids in Kv4.3 are responsible for gating modification by HpTx2, we performed alanine-scanning mutagenesis on amino acids in S3b from positions 273 to 285, and 287 (286 is alanine; Fig. 1). This approach removes the side chain of each amino acid past the β-carbon of each amino acid, thereby limiting disruption of local secondary structure and allowing identification of the amino acids that interact with the toxin (Cunningham and Wells, 1989).

Messenger RNAs for each Kv4.3 mutant were transcribed and expressed in *X. laevis* oocytes. Each construct was tested for sensitivity to HpTx2 using the two-electrode voltage-clamp technique using a two-pulse protocol (see *Materials and Methods*). From a holding potential of −90 mV, voltage was increased to −10 mV (20 mV higher than the activation threshold of Kv4.3) for 3 s to establish the control current amplitude. The two-pulse protocol was initially applied for *X. laevis* oocytes in control solution, and then recombinant HpTx2 was added directly to the flow cell, mixed by gentle pipetting, and the pulse protocol repeated. Currents generated by the alanine mutants had kinetics similar to those of WT Kv4.3, with minor variation in current-voltage, G/G_{max}, and steady-state inactivation relationships (Table 1), suggesting that if these channels possessed the appropriate amino acid binding determinants for HpTx2 interaction, they will show the appropriate gating modification.

The results of the alanine scan are shown in Fig. 2. Gating modification of Kv4.3 by HpTx2 is voltage-dependent (Zarayskiy et al., 2005; Fig. 2, A and B); therefore, we expressed the degree of HpTx2 influence as the difference ($\Delta\Delta G_0$) in the toxin-induced changes in the free energy in G/G_{max} after application of toxin to WT Kv4.3 (see *Materials and Methods*). Positive $\Delta\Delta G_0$ values represent decreased gating modification induced by HpTx2, whereas negative values represent increased gating modification. The alanine mutations that had the largest negative effect on gating were at Leu275 and Val276 (Fig. 2, C, D, and G). Mutating both of these amino acids to alanine resulted in complete elimination of gating modification by HpTx2, identifying Leu275 and Val276 as the critical amino acids necessary for toxin binding to Kv4.3 (Fig. 2G).

HpTx2 is related to HaTx; 64% of their amino acids are either identical or conservative substitutions. Whereas HpTx2 is specific for Kv4 channels, HaTx inhibits both Kv2.1 and Kv4.2 (Swartz and MacKinnon, 1995; Zarayskiy et al., 2005). HaTx binding to Kv2.1 is dependent on three amino acids

TABLE 1

Characterization of Kv4.3 mutants in the presence of 5 μM HpTx2

G/G_{max} and steady-state inactivation relationships were measured as described under *Materials and Methods*. All values are expressed as means ± S.E.M. ($n = 4$).

Channel	Apparent K_d	G/G_{max}					Steady-State Inactivation			
		Control		+ 5 μM HpTx2		ΔG_0	Control		+ 5 μM HpTx2	
		$V_{1/2}$	k	$V_{1/2}$	k		$V_{1/2,i}$	k_i	$V_{1/2,i}$	k_i
	μM	mV		mV		kcal/mol	mV		mV	
WT Kv4.3	1.6–2.3[a]	4.2 ± 1.0	15.0 ± 0.2	29.3 ± 1.6	13.6 ± 1.1	1.9 ± 0.2	−38.7 ± 1.6	4.6 ± 0.1	−17.4 ± 2.2	7.0 ± 0.3
I273A	N.D.	6.4 ± 1.1	16.0 ± 0.3	27.6 ± 1.1	13.4 ± 0.4	1.7 ± 0.1	−46.3 ± 0.2	5.1 ± 0.2	−26.0 ± 0.5	7.2 ± 0.2
G274A	N.D.	3.1 ± 0.8	15.6 ± 0.2	22.5 ± 1.0	15.5 ± 0.2	1.3 ± 0.06	−39.9 ± 0.5	4.8 ± 0.06	−27.3 ± 1.0	8.0 ± 0.5
L275A	25	5.2 ± 0.7	14.3 ± 0.2	10.6 ± 1.4	15.3 ± 0.08	0.3 ± 0.08	−36.9 ± 0.3	4.5 ± 0.1	−34.2 ± 0.3	5.1 ± 0.1
V276A	6.4	2.0 ± 2.3	15.3 ± 0.08	18.0 ± 3.1	15.3 ± 0.7	1.1 ± 0.08	−47.0 ± 7.7	4.6 ± 0.7	−32.6 ± 1.2	6.4 ± 0.1
M277A	N.D.	3.0 ± 1.2	15.6 ± 0.08	26.5 ± 0.3	12.7 ± 0.2	1.9 ± 0.07	−40.1 ± 1.7	4.2 ± 0.8	−17.4 ± 1.1	7.4 ± 0.6
T278A	N.D.	7.0 ± 1.1	14.2 ± 0.4	34.9 ± 4.4	12.9 ± 1.3	2.4 ± 0.5	−35.5 ± 0.7	4.8 ± 0.3	−8.3 ± 6.9	6.7 ± 0.4
N279A	N.D.	11.6 ± 1.3	15.0 ± 0.5	32.5 ± 0.9	11.4 ± 0.4	2.1 ± 0.1	−36.9 ± 2.7	5.1 ± 0.3	17.7 ± 2.4	6.9 ± 0.8
N280A	0.26	7.9 ± 1.6	14.9 ± 0.2	54.9 ± 1.2	11.1 ± 1.0	4.5 ± 0.4	−36.0 ± 1.7	5.9 ± 0.2	−13.9 ± 2.8	6.9 ± 0.3
E281A	N.D.	6.8 ± 0.4	13.4 ± 0.4	35.8 ± 2.4	14.8 ± 1.7	2.1 ± 0.4	−32.9 ± 1.4	4.8 ± 0.4	−2.1 ± 1.7	6.9 ± 0.5
D282A	N.D.	2.1 ± 1.3	14.6 ± 0.1	44.2 ± 4.2	16.6 ± 1.1	2.6 ± 0.5	−45.1 ± 0.4	4.9 ± 0.1	−14.1 ± 1.1	8.7 ± 0.8
V283A	N.D.	−13.1 ± 3.2	19.3 ± 0.6	16.3 ± 3.3	18.2 ± 0.8	1.6 ± 0.08	−57.6 ± 0.8	5.6 ± 0.3	−37.4 ± 2.4	9.0 ± 0.3
S284A	N.D.	5.0 ± 1.2	13.9 ± 0.6	31.0 ± 0.7	13.9 ± 0.6	1.9 ± 0.1	−38.0 ± 3.4[b]	5.0 ± 0.5[b]	−20.1 ± 4.0[b]	7.7 ± 1.7[b]
G285A	N.D.	−5.6 ± 2.2	16.7 ± 0.4	27.6 ± 1.3	15.0 ± 0.5	2.2 ± 0.03	−51.2 ± 2.2	5.2 ± 0.2	−25.9 ± 4.0	11.9 ± 0.6
F287A	N.D.	−2.6 ± 1.7	20.5 ± 0.4	22.9 ± 1.3	13.2 ± 0.3	1.9 ± 0.08	−67.6 ± 1.3	6.6 ± 0.1	−28.7 ± 2.5	7.0 ± 0.5
LV275AA	>70	7.6 ± 1.8	14.6 ± 0.4	7.0 ± 2.0	15.2 ± 0.4	−0.06 ± 0.04	−35.2 ± 1.0[b]	4.6 ± 0.2[b]	−33.8 ± 1.3[b]	4.3 ± 0.9[b]

N.D., not determined.
[a] Determined by independent methods described in Figs. 2 and 3.
[b] $n = 3$.

in S3b: Ile273, Phe274, and Glu277 (Swartz and MacKinnon, 1997b). The positions of the bulky hydrophobic amino acids, leucine and valine in the case of Kv4.3 and isoleucine and phenylalanine in the case of Kv2.1, are conserved between the two channels (Fig. 1). Our scan failed to identify an acidic amino acid requirement for HpTx2 interaction with Kv4.3, suggesting that the identity of the hydrophobic amino acids in Kv4.3 might be critical. To test this idea, we mutated Leu275 and Val276in Kv4.3 to isoleucine and phenylalanine (LV275IF), respectively. It is noteworthy that this mutant increased toxin inhibition of Kv4.3 3-fold at −10 mV (Fig. 3C), suggesting that the hydrophobic character of these amino acids is the key property in HpTx2 interaction. There is an asparagine in Kv4.3 three amino acids downstream from Val276 (analogous to Kv2.1 Glu277; Fig. 1); however, mutation of Asn279 to alanine had little effect on HpTx2 gating modification of Kv4.3 (Fig. 2G). Alanine mutations in two acidic Kv4.3 S3b amino acids, Glu281 and Asp282, did not result in decreased gating modification (Fig. 2G). These data show that the putative HpTx2 binding site consists solely of two hydrophobic amino acids in S3b within the well characterized site for interaction of ICK gating modifier toxins in voltage-gated ion channels.

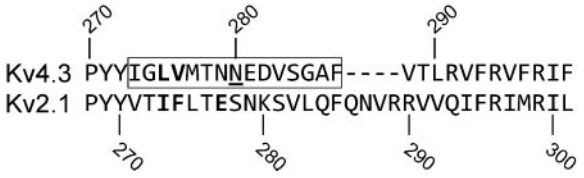

Fig. 1. Sequence alignment of S3b–S4 regions of two mammalian voltage-gated K^+ channel α-subunits, Kv4.3 and Kv2.1. Boxed amino acids are those used in alanine-scanning mutagenesis. Those in boldface type were shown to have the largest decrease of HpTx2 gating modification of Kv4.3 (Fig. 2) or HaTx interaction with Kv2.1 (Swartz and MacKinnon, 1997b). The underlined amino acid is Asn280, which when mutated to alanine was shown to have the largest increase of gating modification by HpTx2 (see Fig. 2G).

Determination of the Dissociation Constant for HpTx2·Kv4.3 and Its Mutants. To quantify the effect of Kv4.3 mutations on interaction with HpTx2, we determined the K_d value for WT Kv4.3 and several of the Kv4.3 S3b mutants at toxin concentrations between 1 nM and 10 μM HpTx2. We used a method previously used with the gating-modifier toxins HaTx, *Scodra griseipes* toxin (SGTx), and APETx1 (Lee et al., 2003; Zhang et al., 2007). Like HpTx2, these toxins all interact with the S3b region of a voltage-gated K^+ channel; Kv2.1 in the case of HaTx and SGTx, Kv11.1 (human *ether-à-go-go*-related gene) with APETx1. The four S3b regions in a tetrameric voltage-gated K^+ channel are approximately 65 Å apart, whereas HpTx2 is 17 Å in its longest dimension, suggesting that there are four toxin binding sites per channel, one in each subunit (Bernard et al., 2000; Long et al., 2005). This method measures the change in degree of gating modification in response to toxin and assumes that it is reflective of the degree of HpTx2 binding.

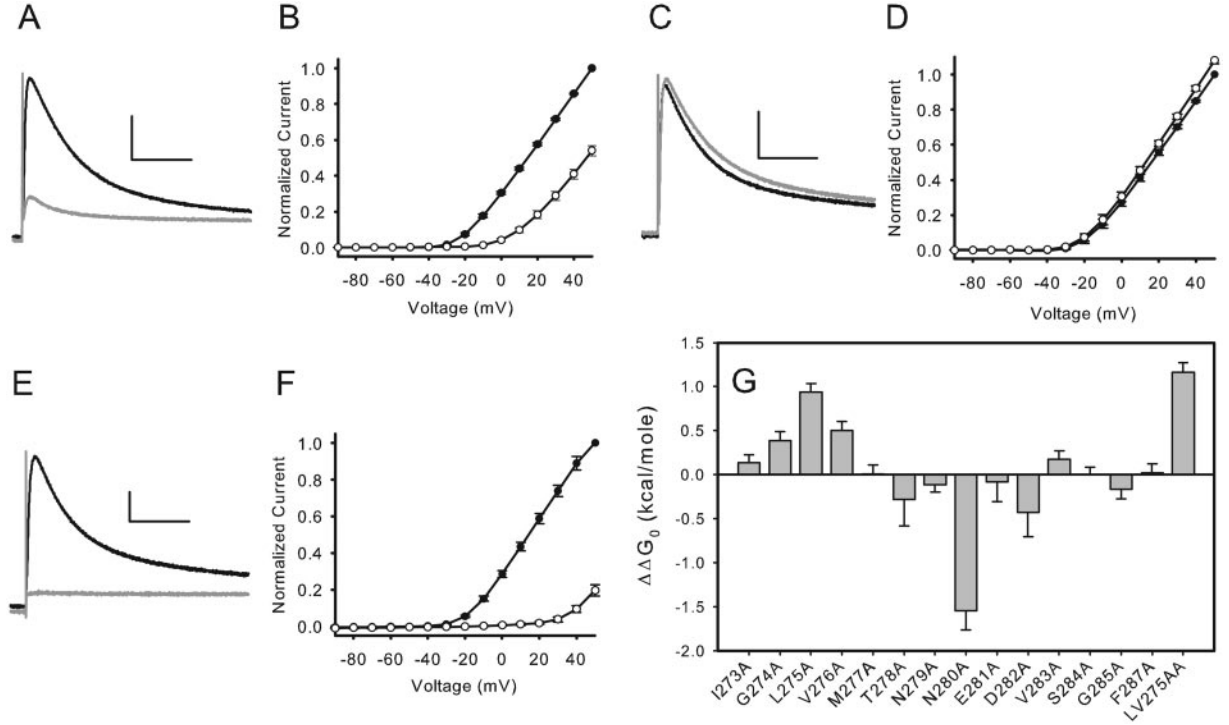

Fig. 2. Inhibition of Kv4.3 mutant channels in the presence of 5 μM HpTx2. A, current traces of Kv4.3 in the presence of 5 μM rHpTx2 in ND96 + 0.1% BSA at −10 mV. The horizontal scale bar is 0.5 s; the vertical scale bar is 0.5 μA. The black trace is the control before toxin application; the gray trace was acquired in the presence of toxin. B, current-voltage relationship of Kv4.3 in the presence of 5 μM rHpTx2 (●, control ± S.E.M., ○, are with toxin ± S.E.M., $n = 4$). C, current traces of Kv4.3 [LV275AA] + 5 μM HpTx2 shows no effect; notations are the same format as in A. D, current-voltage relationships of Kv4.3 [LV275AA] in the presence of 5 μM rHpTx2; notations are the same as in B. E, current traces of Kv4.3 [N280A] shows that HpTx2 has a larger effect on Kv4.3 channel gating; notations are the same as in A. F, current-voltage relationships of Kv4.3 [N280A] in the presence of 5 μM rHpTx2; notations are the same as in B. G, summary of alanine scanning mutagenesis experiments conducted from Ile273 in S3b to Phe287 in the S3b-S4 region of Kv4.3. The $V_{1/2}$, slope, and $\Delta\Delta G_0$ values were calculated from G/G_{max} as described under *Materials and Methods* and as shown in Table 1. The amino acid substitutions with the greatest negative effect on toxin binding are L275A and V276A; the double mutant, LV275AA, nearly eliminated effects due to HpTx2 interaction. N280A had a large negative $\Delta\Delta G_0$, suggesting increased affinity for HpTx2.

However, in the absence of direct binding data, the K_d values reported should be considered apparent K_d values.

The fraction of current inhibited by toxin (I/I_o) was well fit to a function of four independent and equivalent binding sites. As shown in Fig. 2A, strong depolarizations cause channels to open even when bound to toxin (Phillips et al., 2005); therefore currents are measured in response to weak depolarizing pulses in which the assumption is that Kv4.3, with at least one bound toxin, still shows measurable gating modification. To determine the proper "threshold depolarization voltage" (Swartz and MacKinnon, 1997a), oocytes expressing Kv4.3 were subjected to a series of 12-ms voltage pulses from −90 to +50 mV applied from a holding potential −90 mV in 10-mV increments, followed by a step to −90 mV for 150 ms. Fractional occupancy of the channel by HpTx2 was measured by dividing the current amplitude in the presence of 5 μM HpTx2 by the current amplitude of the control. Deactivation of Kv4.3 is relatively fast (Wang et al., 2004) and is accelerated by HpTx2. Therefore, the measurements were performed in 98 mM K^+, which increased the tail current amplitude at negative voltages and slowed the current decay. Based on these measurements, we determined that −10 mV was the optimal depolarization voltage for K_d determination (Fig. 3, A and B).

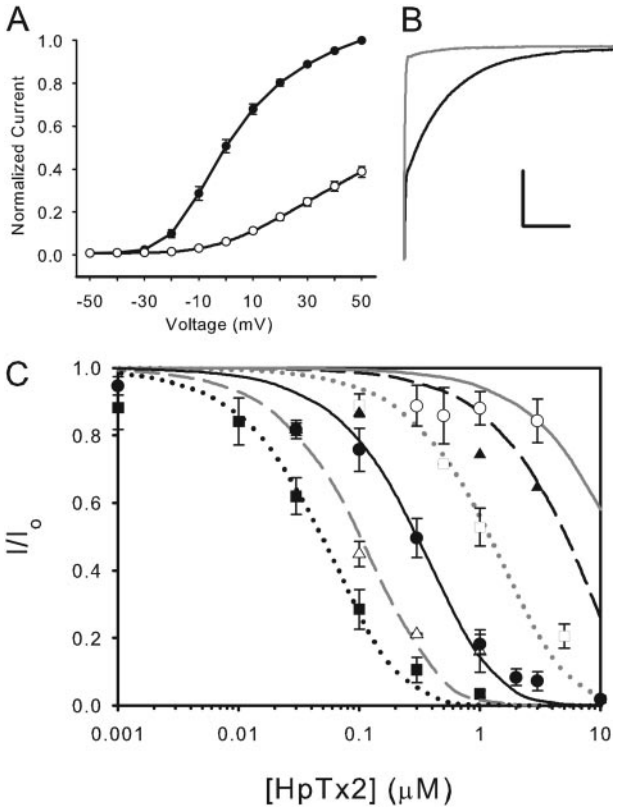

Fig. 3. Dose-response relationship of Kv4.3 and mutant channels. A, determination of the threshold depolarization voltage. Pulse protocol: from a holding potential of −90 mV, voltage was increased to a P1 voltage from −50 to +50 mV in 10-mV increments for 12 ms before subsequent repolarization back to −90 mV. Current amplitude was measured at 43 ms after the end of the P1 pulse and normalized to the maximum current amplitude when P1 = +50 mV. ●, control ± S.E.M.; ○, 1 μM HpTx2 ± S.E.M., $n = 5$. B, raw current traces of Kv4.3 in the presence (gray line) and absence (black line) of 1 μM HpTx2 immediately after the end of a −10 mV P1 pulse; the scale is 2 μA vertically and 10 ms horizontally. C, dose-response of select Kv4.3 constructs to HpTx2 plotted as fractional occupancy (I/I_o) at different concentrations of rHpTx2. The lines are the fits of the fractional occupancies as described in the text; shown are Kv4.3 [N280A] (■), Kv4.3 [LV275IF] (△), wild-type Kv4.3 (●), Kv4.3 [V276A] (□), Kv4.3 L275A (▲), and Kv4.3 [LV275AA] (○). All points are ± S.E.M., with $n = 5$. The apparent K_d values are listed in Table 1.

The protocol described above was applied to Kv4.3 and several of the Kv4.3 mutants at toxin concentrations ranging from 1 nM to 10 μM. The dose-response curves were fit using the equation $I/I_o = (1 - ([HpTx2]/([HpTx2] + K_d))^4$ (Fig. 3C), with a Hill coefficient of 4, assuming four equal and independent binding sites on the channel. This method generated an apparent K_d value of 1.6 μM for wild-type Kv4.3. The mutants that caused the largest positive shift of $\Delta\Delta G_0$ in Fig. 2G, as expected, and gave considerably higher dissociation constants. The apparent K_d values were 6.4 and 25 μM for Kv4.3 [V276A] and Kv4.3 [L275A], respectively. For the Kv4.3 [LV275AA] double mutant, the K_d value was >70 μM. These correspond to $|\Delta\Delta G|$ for channel-toxin binding of 0.8 kcal/mol for Kv4.3 [V276A] and 1.6 kcal/mol for L275A. These values are well within the range expected for the hydrophobic interactions for which these two amino acids are most likely responsible (Thorn and Bogan, 2001).

Several of the Kv4.3 S3b alanine mutants seemed to have higher affinity for HpTx2 than did wild-type Kv4.3. Most significant in this regard is Kv4.3 [N280A]. Our dose-response results showed that the apparent K_d value of this mutant is 0.26 μM, roughly an order of magnitude lower than the K_d value of wild-type Kv4.3; this corresponds to a $\Delta\Delta G$ of −1.2 kcal/mol. The reason for the increase in binding affinity is unclear. The logic of alanine substitution is that it removes only the β-carbon chain of the amino acid, asparagine 280 in this case, while limiting the introduction of secondary conformational and physiochemical changes (Cunningham and Wells, 1989). This suggests that the removal of the glutamine side chain relieved steric inhibition for HpTx2 access to its binding site and perhaps allowed the formation of further interactions within S3b. However, the direct interaction of HpTx2 with the alanine introduced at position 280 cannot be ruled out.

We encountered many technical difficulties measuring accurate dose-response relationships of HpTx2 affinity for Kv4.3. These included the determination of small current amplitudes at low threshold voltages, the oocytes' tendency to produce very high leaks in response to toxin concentration greater than 10 μM, and variations among oocytes in responsiveness to HpTx2. Therefore, to check the accuracy of our dose-response analysis, we used an alternative technique for K_d value determination. We measured the time course for HpTx2 inhibition of Kv4.3 current (τ_{on}) and the time course for release of inhibition after washout of the toxin (τ_{off}). The pulse protocol and solution conditions were similar to those used in Fig. 3C. Figure 4 shows the time course of inhibition during application of 2 μM HpTx2 and after washout. The inhibition data were best fit to the equations $f_{on}(t) = C1(exp(-t/\tau_{on}))$, and the recovery from inhibition by a fourth power function, $f_{off}(t) = C2(1 - \exp(-t/\tau_{off}))^4$; this gave $k_{on} = 1/(4[HpTx2]\tau_{on}) = 8.5 \pm 1.0$ ms/μM and $k_{off} = 1/\tau_{off} = 19.0 \pm 0.1$ ms. Determined by this method, the apparent K_d value was 2.3 ± 0.3 μM, which is in reasonable agreement with our previous estimate of 1.6 μM using the dose-response relationship.

HpTx2 Has a Higher Affinity for the Kv4.3-KChIP2b Complex. *H. venatoria* toxins have frequently been used to

study Kv4-based K^+ currents in vivo (Sanguinetti et al., 1997; Brahmajothi et al., 1999; Guo et al., 1999, 2005; Himmel et al., 1999; Kassiri et al., 2002; Ramakers and Storm, 2002; Sanchez et al., 2002; Varga et al., 2004; Aimond et al., 2005; Tang et al., 2005; Lauver et al., 2006; Wang and Schreurs, 2006; Wang et al., 2006; Colinas et al., 2008; Nerbonne et al., 2008). In general, these studies used toxin concentrations of 100 to 200 nM, which in our assay would produce an approximately 20% decrease in Kv4.3 current at +50 mV (Zarayskiy et al., 2005). Examination of experiments performed on native currents suggested that the IC_{50} value may be much lower than the values we have shown, up to 10-fold in some cases (Sanguinetti et al., 1997; Brahmajothi et al., 1999; Guo et al., 1999; Ramakers and Storm, 2002; Sanchez et al., 2002; Aimond et al., 2005). One factor in this apparent discrepancy could be the presence of Kv4.3 ancillary subunits in native tissues. Therefore, we expressed KChIP2b, a cytoplasmic protein that may participate in cardiac I_{to} (Patel et al., 2002), with Kv4.3 in *X. laevis* oocytes and tested its response to application of HpTx2.

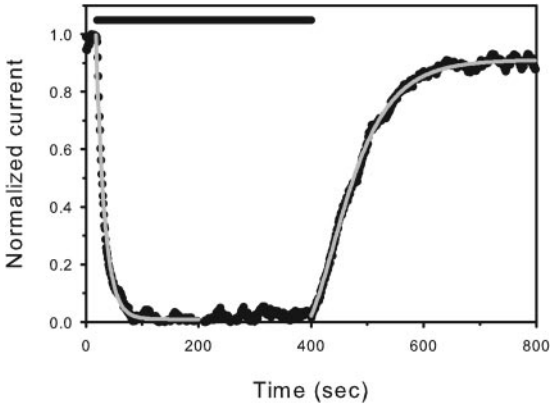

Fig. 4. Time course of inhibition of Kv4.3 with 2 μM HpTx2 and recovery from inhibition. The bar indicates the duration of 2 μM HpTx2 application. The two pulse protocol started from a holding potential of −90 mV; the P1 pulse was to −10 mV for 12 ms, followed by a P2 pulse to −50 mV for 150 ms, followed by a 1-s interpulse interval. The data represent the normalized reciprocal current amplitude measured from the P2 pulse. The experiment was performed in 98 mM KCl solution (see *Materials and Methods*) to maximize current amplitude. Gray lines show the fits with the functions $f_1(t) = C1[\exp(-4\ k_{on(t)}]$ for τ_{on} and $f_2(t) = C2[1 - \exp(-k_{off} \cdot t)]^4$ for τ_{off}.

As we have previously shown (Bett et al., 2006; Li et al., 2006), KChIP2b coexpression slows the major component of Kv4.3 inactivation, causes a negative shift in the $V_{1/2}$ of steady-state inactivation, and speeds recovery from inactivation (Fig. 5). We found that KChIP2b also increases the inhibition of Kv4.3 K^+ current by HpTx2. At +50 mV, 2 μM HpTx2 decreases Kv4.3 current by 31% (Fig. 5, A to C); however, expression with KChIP2b increases inhibition to 49% of current in the presence of toxin (Fig. 5, A–C). The increased inhibition is apparent at all voltages (Fig. 5C). We determined the K_d value of Kv4.3 + KChIP2b by the method established in Fig. 4. The k_{off} was the same as was measured for Kv4.3 alone, 20.0 ± 1.0 ms. However, the k_{on} = 2.3 ± 0.1 ms/μM, resulting in a K_d value that is 2.4 times lower at 0.95 ± 0.11 μM (Fig. 6).

The structure of the cytoplasmic KChIP/Kv4 T1 domain complex has been determined (Pioletti et al., 2006; Wang et al., 2007). One important implication of these studies is that the KChIPs are sequestered away from the inner membrane,

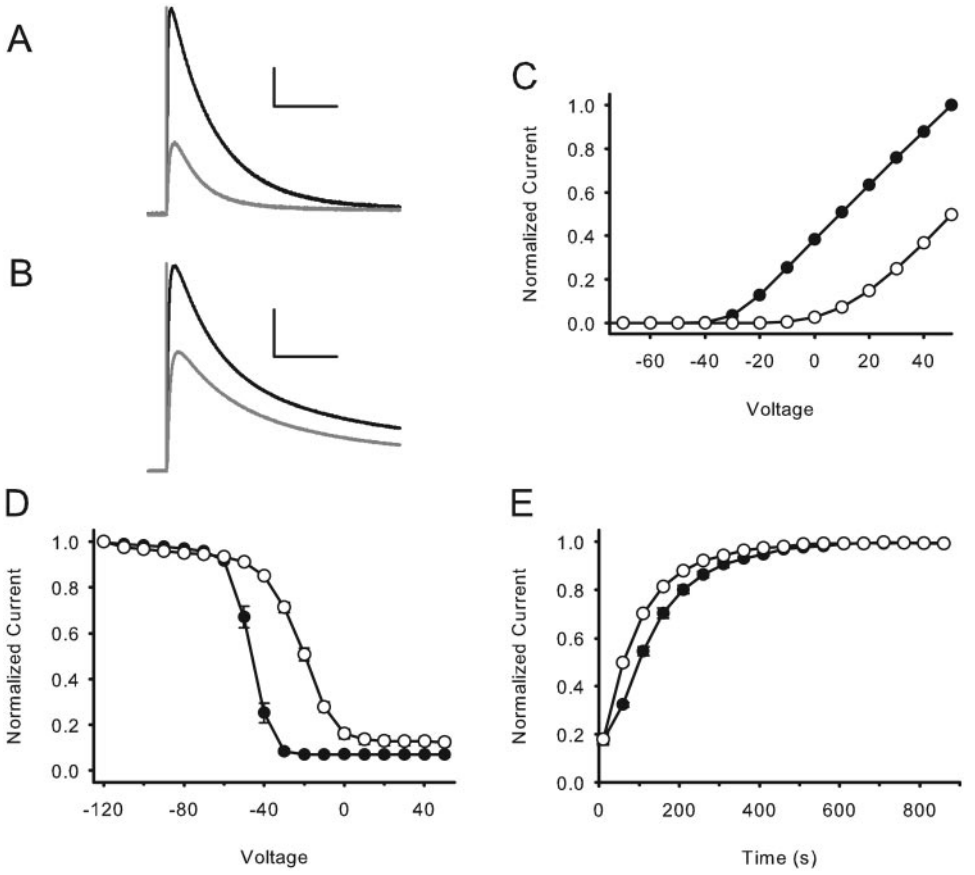

Fig. 5. The influence of KChIP2b expression with Kv4.3 on HpTx2 interaction. Raw current traces measured at +30 mV in control (black traces) and in the presence of 2 μM HpTx2 (gray traces). A, Kv4.3 coexpressed with KChIP2b; the scale bar is 1 μA vertically and 0.5 s horizontally. B, Kv4.3 alone; the scale bar is 2 μA vertically and 0.5 s horizontally. Current voltage relationship (C), steady-state inactivation (D), relationships (D), and recovery from inactivation (E) of Kv4.3 + KChIP2b in response to 2 μM HpTx2 (● and ○ represent measurements in the absence and in the presence of toxin, respectively); all data shown as ± S.E.M., n = 5.

making it unlikely that KChIPs have direct contact with the cytoplasmic loops of the transmembrane segments, including S3, which we have established as the HpTx2 interaction site. The T1 domain to which KChIPs are complexed is a conserved region among the Kv1–Kv4 families that consists of approximately 100 amino acids in a highly ordered cytoplasmic structure (Kreusch et al., 1998). It is responsible for assembly specificity within a family, is a binding site for several ancillary subunits (including KChIPs), controls subcellular localization, and modulates gating (Maffie and Rudy, 2008). The T1 domain's structure and role in gating and localization suggest that KChIPs might influence the S3 transmembrane domain allosterically, thereby revealing additional binding determinants on S3 or elsewhere. To test this hypothesis, we expressed Kv4.3 [LV275AA], the mutant that was not inhibited by HpTx2, with KChIP2b. There was no detectable inhibition upon application of 5 μM HpTx2 (Fig. 6B), showing that no additional binding determinants were uncovered by association with KChIP2b. This suggests that the increase in gating modification caused by KChIP2b is due to its effects on the kinetics of Kv4.3 gating and further supports that LV275 are the critical amino acids for HpTx2 binding to Kv4.3.

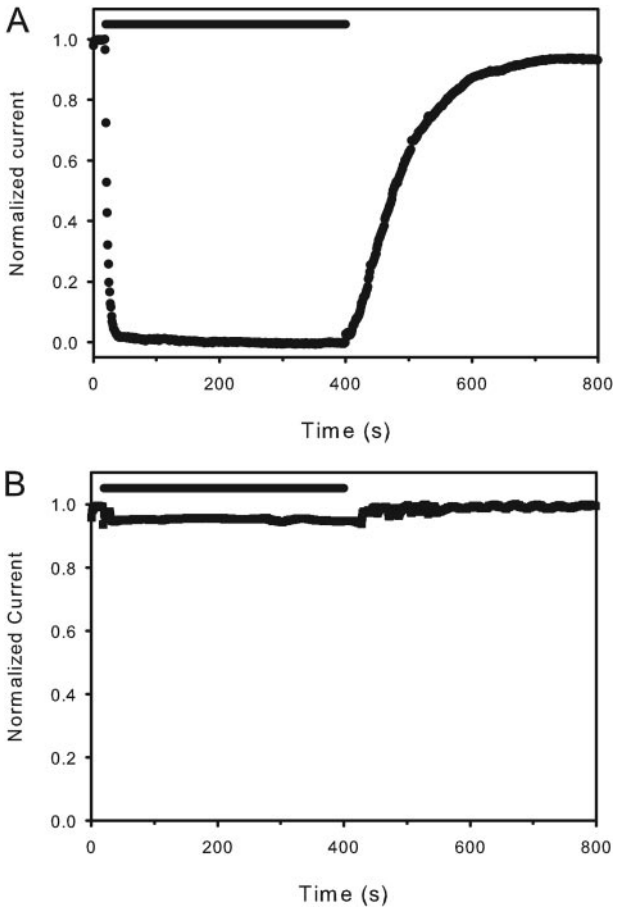

Fig. 6. Time course of inhibition of Kv4.3 and Kv4.3 [LV275AA] coexpressed with KChIP2b by 2 μM rHpTx2 and recovery from inhibition. The bar indicates the duration of 2 μM HpTx2 application. A, WT Kv4.3 + KChIP2b; the apparent K_d value was 0.95 ± 0.3 μM, calculated as described in Fig. 4. B, Kv4.3 [LV275AA] + KChIP2b had no significant affinity for 2 μM HpTx2.

Discussion

We used alanine scanning mutagenesis of Kv4.3 combined with electrophysiological assays to localize the site responsible for HpTx2-induced gating modification. Mutation of Leu275 and Val276 in S3b resulted in the complete elimination of gating modification, identifying them as the critical amino acids in Kv4.3 for HpTx2 interaction. Although we cannot completely rule out that an alanine scan extended to adjacent parts of the channel might reveal mutations that influence toxin binding, the nearly complete loss of gating modification in Kv4.3 [LV275AA], combined with the mutant channels' normal gating properties (Table 1), suggest that these two amino acids are necessary for HpTx2 binding. These bulky, hydrophobic amino acids are in the same position in Kv4.3 as the isoleucine and phenylalanine in Kv2.1 required for HaTx interaction; however, unlike HaTx, HpTx2 has no requirement for an acidic amino acid.

HpTx2 joins a growing list of peptide-gating modifier toxins that interact with the outer portion of S3 or the S3–S4 linker of voltage-gated ion channels (Catterall et al., 2007; Swartz, 2007; Bosmans et al., 2008; Norton and McDonough, 2008). In several cases, careful channel mutagenesis studies have been performed. These studies have shown that the toxin binding sites are often complex and are dependent on either a combination of charged and hydrophobic amino acids or charge interactions alone (Swartz and MacKinnon, 1997b; Alabi et al., 2007; Catterall et al., 2007; Smith and Blumenthal, 2007; Swartz, 2007; Zhang et al., 2007; Bosmans et al., 2008; Norton and McDonough, 2008). HpTx2 is thus far unique among the ICK toxins in relying solely on hydrophobic contacts for channel interaction.

The paradigm for gating-modifier ICK peptide toxins is HaTx (Swartz and MacKinnon, 1995). HaTx and HpTx2 share 40% primary sequence identity and 63% with respect to conserved amino acid properties. Although HpTx2 is specific for Kv4 channels, HaTx has been shown to inhibit Kv2.1 and Kv4.2 to similar extents (Swartz and MacKinnon, 1995; Swartz, 2007). Despite these similarities, HaTx has been shown to have three major binding determinants within Kv2.1 S3b: two hydrophobic amino acids analogous to LV275 in Kv4.3, plus a glutamic acid just downstream (Fig. 1). As might be expected from the additional interaction, the 300 nM K_d value for HaTx·Kv2.1 is lower than that for interaction of HpTx2 with Kv4.3 (Milescu et al., 2007).

It is perhaps unsurprising that HpTx2 lacks an acidic binding determinant on the channel; the net charge of the 35-amino acid HaTx is +2, but HpTx2 is more acidic, with a net charge of −3 over its 32 amino acids (Sanguinetti et al., 1997). Mutation of LV275 to the isoleucine and phenylalanine in Kv4.3 found in Kv2.1 reduced the K_d value of HpTx2 to a value near that of HaTx inhibition of Kv2.1, suggesting that the main difference in affinity is due to the extent of hydrophobic interactions.

In addition to the LV275IF mutation, we discovered other conditions in which the K_d of HpTx2 was decreased. One of these was coexpression of the Kv4.3 ancillary subunit, KChIP2b. The effects of KChIP2b on Kv4.3 have been studied in detail (Patel et al., 2002, 2004; Wang et al., 2002; Bett et al., 2006). KChIP2b causes small shifts in steady-state activation and deactivation and slows both open and closed-state inactivation kinetics considerably. Its most significant

effects are a shift of approximately −5 mV in the $V_{1/2}$ of steady-state inactivation and a 4-fold increase in the rate of recovery from inactivation.

We found that HpTx2 had a K_d value for Kv4.3+KChIP2b of 0.95 ± 0.11 μM, 2.4 times less than the K_d value with Kv4.3 alone. However, HpTx2 caused no apparent difference in activation, deactivation, inactivation, or recovery kinetics that was dependent on KChIP2b expression. We tested the possibility that the increased affinity could be due to exposure of additional binding determinants in S3b through allosteric effects of KChIP2b on the inside of the channel. However, the Kv4.3 [LV275AA] mutation had little apparent affinity for toxin in the presence of KChIP2b.

What is the reason for the enhanced affinity of the Kv4.3·KChIP2b complex? The negative shift in steady-state inactivation and fast recovery from inactivation are manifestations of KChIP2b stabilizing the closed state of Kv4.3. Like the gating modifier toxins HaTx, SGTx, and APETx1, HpTx2 binds to Kv4.3 in its closed state (Lee et al., 2003; Zhang et al., 2007; DeSimone, 2008). Therefore, agents that stabilize the closed state such as KChIP2b would be predicted to increase the affinity of HpTx2 for Kv4.3. Moreover, HpTx2 speeds deactivation of Kv4.3, further stabilizing the closed state. Superimposing the increased stabilization of the closed state by KChIP2b and HpTx2 increases gating modification of Kv4.3 and the calculated apparent K_d value. Kv4 channels in vivo are associated with several types of ancillary subunits, many of which speed recovery and therefore stabilize the closed state of the channel (Patel et al., 2004).

The increase in gating modification shown when HpTx2 is applied to Kv4.3 coexpressed with KChIP2b in *X. laevis* oocytes does not seem to fully recapitulate the increased affinity that seems to be evident in native Kv4-based transient outward K^+ currents. There are several possible explanations for this observation, including the presence of additional ancillary subunits or differences in the membrane lipid composition in *X. laevis* oocytes compared with cardiomyocytes or neurons. However, our data do provide a partial explanation for the apparent differences seen in response to HpTx2 between native and heterologously expressed K^+ currents. We suggest that when applied to native transient K^+ currents based on Kv4 channels, HpTx2 will be more potent than we have found for Kv4.3 expressed in oocytes in the absence of ancillary subunits (Sanguinetti et al., 1997; Brahmajothi et al., 1999; Guo et al., 1999; Himmel et al., 1999; Ramakers and Storm, 2002; Sanchez et al., 2002; Varga et al., 2004; Tang et al., 2005; Lauver et al., 2006; Wang and Schreurs, 2006; Colinas et al., 2008).

These findings have important implications in consideration of toxins like HpTx2 as scaffolds for rational drug design. Drug binding can be influenced profoundly by the presence of ancillary subunits (Bett and Rasmusson, 2008). KChIP2b alters the use-dependence and potency of the common antiarrhythmic nifedipine, rendering it potentially less effective in vivo than would be predicted from studies of Kv4.3 (Bett et al., 2006). However, because of their enhanced affinity for the closed state, drugs that mimic the actions of spider toxins may be more effective than many compounds in current use when the presence of ancillary subunits is taken into account.

A final intervention that increased toxin affinity for Kv4.3 was the N280A mutation: the apparent K_d value was nearly 10-fold lower than that measured with wild-type Kv4.3. It is unlikely that the cause of this increased affinity is due to the mutant stabilizing the closed state of Kv4.3, because we observed no kinetic differences such as faster recovery from inactivation that would suggest this. Instead, it is likely that removal of the asparagine side chain removes a steric hindrance to toxin interaction with S3b.

An interesting difference between HpTx2 and most other ICK toxins, including HaTx, is the discrepancy in their affinity for membrane lipid bilayers. Several ICK toxins, including HaTx, have been shown to have affinity for phospholipid vesicles, an effect that could decrease the K_d value of an ICK toxin for its target approximately 1 order of magnitude (Lee and MacKinnon, 2004; Phillips et al., 2005; Smith et al., 2005; Milescu et al., 2007; Posokhov et al., 2007; Zeng et al., 2007). However, HpTx2 and huwentoxin IV (an ICK toxin inhibitor of neuronal Na^+ channels) have no apparent affinity for membranes (Posokhov et al., 2007; Xiao et al., 2008). It has been suggested that membrane partitioning may be obligatory for spider toxin binding to voltage-gated cation channels (Lee and MacKinnon, 2004; Milescu et al., 2007). This implies that the binding site for these toxins in the voltage-sensor domain of the channel is submerged in the membrane (Lee and MacKinnon, 2004; Alabi et al., 2007; Long et al., 2007; Milescu et al., 2007). Although partition of toxin into the membrane would concentrate the toxin near its binding site, thereby increasing its effective concentration (Milescu et al., 2007), the examples of HpTx2 and huwentoxin IV show that membrane interaction is not obligatory. It has been suggested that HpTx2 membrane interaction lower than the limit of detection could still result in significant concentrations of toxin in the membrane (Milescu et al., 2007; Posokhov et al., 2007). We argue that this is not the case. The difference in K_d values between HpTx2 and HaTx only accounts for a difference in binding free energy of ≃1 kcal/mol; this can easily be accounted for by the additional salt bridge present with the extra HaTx binding determinant, Kv2.1 glutamic acid 277 (Fig. 1). Furthermore, we are able reduce the K_d value of HpTx2 to a value comparable with that of HaTx with either the Kv4.3 [LV275IF] or [N280A] mutations. We do not dispute the importance of lipid bilayer interactions for channel binding of many ICK toxins; however, it is unlikely to be a factor in the interaction of HpTx2 with Kv4.3. Instead, we suggest that the voltage-sensor domain of Kv4.3 has a slightly different resting conformation with respect to the membrane so that its toxin binding site is accessible without membrane interaction. Testing of this hypothesis will have to await structural determination of the channel toxin complex.

Acknowledgments

We thank Dr. Chang Xie for assistance in preparation of oocytes and Drs. Harold Strauss and Randall Rasmusson for support and encouragement.

References

Aimond F, Kwak SP, Rhodes KJ, and Nerbonne JM (2005) Accessory Kvβ_1 subunits differentially modulate the functional expression of voltage-gated K^+ channels in mouse ventricular myocytes. *Circ Res* **96:**451–458.

Alabi AA, Bahamonde MI, Jung HJ, Kim JI, and Swartz KJ (2007) Portability of paddle motif function and pharmacology in voltage sensors. *Nature* **450:**370–375.

Bernard C, Legros C, Ferrat G, Bischoff U, Marquardt A, Pongs O, and Darbon H (2000) Solution structure of HpTx2, a toxin from *Heteropoda venatoria* spider that blocks Kv4.2 potassium channel. *Protein Sci* **9:**2059–2067.

Bett GC, Morales MJ, Strauss HC, and Rasmusson RL (2006) KChIP2b modulates

the affinity and use-dependent block of Kv4.3 by nifedipine. *Biochem Biophys Res Commun* **340:**1167–1177.
Bett GC and Rasmusson RL (2008) Modification of K^+ channel-drug interactions by ancillary subunits. *J Physiol* **586:**929–950.
Birnbaum SG, Varga AW, Yuan LL, Anderson AE, Sweatt JD, and Schrader LA (2004) Structure and function of Kv4-family transient potassium channels. *Physiol Rev* **84:**803–833.
Bosmans F, Martin-Eauclaire MF, and Swartz KJ (2008) Deconstructing voltage sensor function and pharmacology in sodium channels. *Nature* **456:**202–208.
Brahmajothi MV, Campbell DL, Rasmusson RL, Morales MJ, Trimmer JS, Nerbonne JM, and Strauss HC (1999) Distinct transient outward potassium current (I_{to}) phenotypes and distribution of fast-inactivating potassium channel alpha subunits in ferret left ventricular myocytes. *J Gen Physiol* **113:**581–600.
Catterall WA, Cestèle S, Yarov-Yarovoy V, Yu FH, Konoki K, and Scheuer T (2007) Voltage-gated ion channels and gating modifier toxins. *Toxicon* **49:**124–141.
Colinas O, Pérez-Carretero FD, López-López JR, and Pérez-García MT (2008) A role for DPPX modulating external TEA sensitivity of Kv4 channels. *J Gen Physiol* **131:**455–471.
Covarrubias M, Bhattacharji A, De Santiago-Castillo JA, Dougherty K, Kaulin YA, Na-Phuket TR, and Wang G (2008) The neuronal Kv4 channel complex. *Neurochem Res* **33:**1558–1567.
Cunningham BC and Wells JA (1989) High-resolution epitope mapping of hGH-receptor interactions by alanine-scanning mutagenesis. *Science* **244:**1081–1085.
DeSimone CV (2008) HpTx2 gating modification involves distinct amino acids in S3b region of Kv4. PhD thesis, University at Buffalo, the State University of New York.
Guo W, Jung WE, Marionneau C, Aimond F, Xu H, Yamada KA, Schwarz TL, Demolombe S, and Nerbonne JM (2005) Targeted deletion of Kv4.2 eliminates $I_{to,f}$ and results in electrical and molecular remodeling, with no evidence of ventricular hypertrophy or myocardial dysfunction. *Circ Res* **97:**1342–1350.
Guo W, Xu H, London B, and Nerbonne JM (1999) Molecular basis of transient outward K^+ current diversity in mouse ventricular myocytes. *J Physiol* **521:**587–599.
Himmel HM, Wettwer E, Li Q, and Ravens U (1999) Four different components contribute to outward current in rat ventricular myocytes. *Am J Physiol* **277:** H107–H118.
Institute of Laboratory Animal Resources (1996) *Guide for the Care and Use of Laboratory Animals* 7th ed. Institute of Laboratory Animal Resources, Commission on Life Sciences, National Research Council, Washington DC.
Jerng HH, Pfaffinger PJ, and Covarrubias M (2004) Molecular physiology and modulation of somatodendritic A-type potassium channels. *Mol Cell Neurosci* **27:**343–369.
Kassiri Z, Zobel C, Nguyen TT, Molkentin JD, and Backx PH (2002) Reduction of I_{to} causes hypertrophy in neonatal rat ventricular myocytes. *Circ Res* **90:**578–585.
Kreusch A, Pfaffinger PJ, Stevens CF, and Choe S (1998) Crystal structure of the tetramerization domain of the *Shaker* potassium channel. *Nature* **392:**945–948.
Lauver A, Yuan LL, Jeromin A, Nadin BM, Rodríguez JJ, Davies HA, Stewart MG, Wu GY, and Pfaffinger PJ (2006) Manipulating Kv4.2 identifies a specific component of hippocampal pyramidal neuron A-current that depends upon Kv4.2 expression. *J Neurochem* **99:**1207–1223.
Lee HC, Wang JM, and Swartz KJ (2003) Interaction between extracellular Hanatoxin and the resting conformation of the voltage-sensor paddle in Kv channels. *Neuron* **40:**527–536.
Lee SY and MacKinnon R (2004) A membrane-access mechanism of ion channel inhibition by voltage sensor toxins from spider venom. *Nature* **430:**232–235.
Li HL, Qu YJ, Lu YC, Bondarenko VE, Wang S, Skerrett IM, and Morales MJ (2006) DPP10 is an inactivation modulatory protein of Kv4.3 and Kv1.4. *Am J Physiol Cell Physiol* **291:**C966–C976.
Long SB, Campbell EB, and Mackinnon R (2005) Crystal structure of a mammalian voltage-dependent *Shaker* family K^+ channel. *Science* **309:**897–903.
Long SB, Tao X, Campbell EB, and MacKinnon R (2007) Atomic structure of a voltage-dependent K^+ channel in a lipid membrane-like environment. *Nature* **450:**376–382.
Maffie J and Rudy B (2008) Weighing the evidence for a ternary protein complex mediating A-type K^+ currents in neurons. *J Physiol* **586:**5609–5623.
Milescu M, Vobecky J, Roh SH, Kim SH, Jung HJ, Kim JI, and Swartz KJ (2007) Tarantula toxins interact with voltage sensors within lipid membranes. *J Gen Physiol* **130:**497–511.
Nattel S and Carlsson L (2006) Innovative approaches to anti-arrhythmic drug therapy. *Nat Rev Drug Discov* **5:**1034–1049.
Nerbonne JM, Gerber BR, Norris A, and Burkhalter A (2008) Electrical remodelling maintains firing properties in cortical pyramidal neurons lacking KCND2-encoded A-type K^+ currents. *J Physiol* **586:**1565–1579.
Norton RS and McDonough SI (2008) Peptides targeting voltage-gated calcium channels. *Curr Pharm Des* **14:**2480–2491.
Norton RS and Pallaghy PK (1998) The cystine knot structure of ion channel toxins and related polypeptides. *Toxicon* **36:**1573–1583.
Patel SP and Campbell DL (2005) Transient outward potassium current, 'I_{to}', phenotypes in the mammalian left ventricle: underlying molecular, cellular and biophysical mechanisms. *J Physiol* **569:**7–39.
Patel SP, Campbell DL, Morales MJ, and Strauss HC (2002) Heterogeneous expression of KChIP2 isoforms in the ferret heart. *J Physiol* **539:**649–656.
Patel SP, Parai R, Parai R, and Campbell DL (2004) Regulation of Kv4.3 voltage-dependent gating kinetics by KChIP2 isoforms. *J Physiol* **557:**19–41.
Phillips LR, Milescu M, Li-Smerin Y, Mindell JA, Kim JI, and Swartz KJ (2005) Voltage-sensor activation with a tarantula toxin as cargo. *Nature* **436:**857–860.
Pioletti M, Findeisen F, Hura GL, and Minor DL Jr (2006) Three-dimensional structure of the KChIP1-Kv4.3 T1 complex reveals a cross-shaped octamer. *Nat Struct Mol Biol* **13:**987–995.
Posokhov YO, Gottlieb PA, Morales MJ, Sachs F, and Ladokhin AS (2007) Is lipid bilayer binding a common property of inhibitor cysteine knot ion-channel blockers? *Biophys J* **93:**L20–L22.
Ramakers GM and Storm JF (2002) A postsynaptic transient K^+ current modulated by arachidonic acid regulates synaptic integration and threshold for LTP induction in hippocampal pyramidal cells. *Proc Natl Acad Sci U S A* **99:**10144–10149.
Sanchez D, López-López JR, Pérez-García MT, Sanz-Alfayate G, Obeso A, Ganfornina MD, and Gonzalez C (2002) Molecular identification of Kvα subunits that contribute to the oxygen-sensitive K^+ current of chemoreceptor cells of the rabbit carotid body. *J Physiol* **542:**369–382.
Sanguinetti MC, Johnson JH, Hammerland LG, Kelbaugh PR, Volkmann RA, Saccomano NA, and Mueller AL (1997) Heteropodatoxins: peptides isolated from spider venom that block Kv4.2 potassium channels. *Mol Pharmacol* **51:**491–498.
Smith JJ, Alphy S, Seibert AL, and Blumenthal KM (2005) Differential phospholipid binding by site 3 and site 4 toxins. Implications for structural variability between voltage-sensitive sodium channel domains. *J Biol Chem* **280:**11127–11133.
Smith JJ and Blumenthal KM (2007) Site-3 sea anemone toxins: molecular probes of gating mechanisms in voltage-dependent sodium channels. *Toxicon* **49:**159–170.
Swartz KJ (2007) Tarantula toxins interacting with voltage sensors in potassium channels. *Toxicon* **49:**213–230.
Swartz KJ and MacKinnon R (1995) An inhibitor of the Kv2.1 potassium channel isolated from the venom of a Chilean tarantula. *Neuron* **15:**941–949.
Swartz KJ and MacKinnon R (1997a) Hanatoxin modifies the gating of a voltage-dependent K^+ channel through multiple binding sites. *Neuron* **18:**665–673.
Swartz KJ and MacKinnon R (1997b) Mapping the receptor site for hanatoxin, a gating modifier of voltage-dependent K^+ channels. *Neuron* **18:**675–682.
Tang SL, Tran V, and Wagner EJ (2005) Sex differences in the cannabinoid modulation of an A-type K^+ current in neurons of the mammalian hypothalamus. *J Neurophysiol* **94:**2983–2986.
Thorn KS and Bogan AA (2001) ASEdb: a database of alanine mutations and their effects on the free energy of binding in protein interactions. *Bioinformatics* **17:** 284–285.
Varga AW, Yuan LL, Anderson AE, Schrader LA, Wu GY, Gatchel JR, Johnston D, and Sweatt JD (2004) Calcium-calmodulin-dependent kinase II modulates Kv4.2 channel expression and upregulates neuronal A-type potassium currents. *J Neurosci* **24:**3643–3654.
Wang D and Schreurs BG (2006) Characteristics of I_A currents in adult rabbit cerebellar Purkinje cells. *Brain Res* **1096:**85–96.
Wang H, Yan Y, Liu Q, Huang Y, Shen Y, Chen L, Chen Y, Yang Q, Hao Q, Wang K, et al. (2007) Structural basis for modulation of Kv4 K^+ channels by auxiliary KChIP subunits. *Nat Neurosci* **10:**32–39.
Wang S, Bondarenko VE, Qu Y, Morales MJ, Rasmusson RL, and Strauss HC (2004) Activation properties of Kv4.3 channels: time, voltage and $[K^+]_o$ dependence. *J Physiol* **557:**705–717.
Wang S, Patel SP, Qu Y, Hua P, Strauss HC, and Morales MJ (2002) Kinetic properties of Kv4.3 and their modulation by KChIP2b. *Biochem Biophys Res Commun* **295:**223–229.
Wang Y, Cheng J, Tandan S, Jiang M, McCloskey DT, and Hill JA (2006) Transient-outward K^+ channel inhibition facilitates L-type Ca^{2+} current in heart. *J Cardiovasc Electrophysiol* **17:**298–304.
Wickenden A (2002) K^+ channels as therapeutic drug targets. *Pharmacol Ther* **94:**157–182.
Xiao Y, Luo X, Kuang F, Deng M, Wang M, Zeng X, and Liang S (2008) Synthesis and characterization of huwentoxin-IV, a neurotoxin inhibiting central neuronal sodium channels. *Toxicon* **51:**230–239.
Zarayskiy VV, Balasubramanian G, Bondarenko VE, and Morales MJ (2005) *Heteropoda* toxin 2 is a gating modifier toxin specific for voltage-gated K^+ channels of the Kv4 family. *Toxicon* **45:**431–442.
Zeng X, Deng M, Lin Y, Yuan C, Pi J, and Liang S (2007) Isolation and characterization of Jingzhaotoxin-V, a novel neurotoxin from the venom of the spider *Chilobrachys jingzhao*. *Toxicon* **49:**388–399.
Zhang M, Liu XS, Diochot S, Lazdunski M, and Tseng GN (2007) APETx1 from sea anemone *Anthopleura elegantissima* is a gating modifier peptide toxin of the human *ether-a-go-go*-related potassium channel. *Mol Pharmacol* **72:**259–268.

Address correspondence to: Dr. Michael J. Morales, Department of Physiology and Biophysics, University at Buffalo, the State University of New York, 124 Sherman Hall, Buffalo, NY 14214. E-mail: moralesm@buffalo.edu